Clay Minerals (2003) **38**, 63–69

^{23}Na 2D 3QMAS NMR and ^{29}Si, ^{27}Al MAS NMR investigation of Laponite and synthetic saponites of variable interlayer charge

L. DELEVOYE[1], J.-L. ROBERT[2] AND J. GRANDJEAN[3]

[1]*Bruker S. A. Solid-state NMR Application Lab., F-67166 Wissembourg, France,* [2]*ISTO, UMR 6113, CNRS - Université Orleans, F-45071 Orléans Cedex 2, France, and* [3]*University of Liege, Institute of Chemistry B6a, COSM, Sart-Tilman, B-4000 Liege, Belgium*

(*Received 15 June 2001; revised 5 June 2002*)

ABSTRACT: ^{29}Si, ^{27}Al MAS NMR is used to characterize Laponite RD and synthetic saponites of variable interlayer charge. The Si/Al ratios are in good agreement with the calculated charge from chemical analysis except for the lowest-charged saponite. In contrast to the ^{29}Si MAS NMR spectra in which resolved signals are detected, the ^{27}Al MAS NMR spectra show one signal whose linewidth increases with the clay charge. The water content of the clay samples was obtained from ^{1}H MAS NMR.

The 2D MQMAS NMR technique is required to obtain a high-resolution spectrum of nuclei with strong quadrupolar interaction. This method was applied to the ^{23}Na nucleus of clay counterions and to the ^{27}Al structural nucleus. One well-defined ^{23}Na NMR signal is observed for all the clays studied except the highest-charged saponite. Possible explanations for this different behaviour are discussed. The calculated isotropic chemical shift evolves progressively with the clay charge whereas the deduced quadrupolar interaction does not change significantly. The ^{27}Al 2D 3QMAS technique was not able to resolve more than one signal.

KEYWORDS: 2:1 phyllosilicate, saponite, Laponite, ^{1}H, ^{23}Na, ^{27}Al and ^{29}Si MAS NMR, 2D 3QMAS NMR.

As part of our investigations on synthetic clay suspensions, we have studied the properties of Na^+ and Li^+ cations that counterbalance the negative charges of clay platelets. The strength of the cation interaction with the solid surface affects its environment, and modulates the interaction of non-ionic (Grandjean & Robert, 1999; Gevers & Grandjean, 2001), and zwitterionic (Grandjean, 2001) surfactants with clays. Surfactant interaction is found with Laponite and low-charge saponites in suspension. Within the saponite series, the interaction decreases with the increase of the clay charge and becomes negligible with the highest investigated charge.

In this paper, we have first considered the influence of the clay charge on the ^{29}Si, ^{27}Al MAS NMR spectra of synthetic saponites. As the interlayer charge was so sensitive to clay-surfactant interaction, we have investigated how the location of cation isomorphous substitution and the clay charge affect the ^{23}Na NMR parameters as defined by 2D 3QMAS NMR (two-dimensional 3 quantum magic angle spinning NMR).

Saponite and Laponite are trioctahedral clays (2:1 phyllosilicates) with all three of their octahedral sites occupied by Mg(II). Clay platelets are negatively charged as a result of cation isomor-

* E-mail: j.grandjean@ulg.ac.be
DOI: 10.1180/0009855033810079

phous substitution either in the octahedral layer (Li(I) for Mg(II) in Laponite) or in the tetrahedral layer (Al(III) for Si(IV) in saponite). Cation isomorphous substitution thus induces negative charges on clay platelets, and exchangeable Na^+ cations occupy the interlamellar space in order to preserve electroneutrality.

Solid-state magic angle spinning (MAS) ^{29}Si and ^{29}Al NMR spectroscopy have been used to study the detailed structure of phyllosilicates (Sanz & Serratosa, 1984; Alma *et al.*, 1984; Kinsey *et al.*, 1985; Herrero *et al.*, 1989; Sanz & Robert, 1992). Thermal or acid treatment on such minerals has been followed by these methods (Mandair *et al.*, 1990; McKenzie & Meinhold, 1994; Tkáč *et al.*, 1994; Komadel *et al.*, 1996). The perturbation brought by Fe centres on ^{29}Si and ^{29}Al NMR spectra has been investigated in kaolinite (Schroeder & Pruett, 1996). The state of counterions in clays has been described from MAS spectra of relevant nuclei such as ^{7}Li, ^{23}Na, ^{39}K, ^{111}Cd and ^{133}Cs (Luca *et al.*, 1989; Laperche *et al.*, 1990; Lambert *et al.*, 1992; Kim & Kirkpatrick, 1997; Kim *et al.*, 1996).

The spin quantum number I is equal to 1/2 for dipolar nuclei (^{29}Si, ^{111}Cd). When I is >1/2, the nucleus is characterized by an electric quadrupole moment that interacts with the electric field gradient generated by the environment at the nucleus site. This quadrupolar interaction splits the NMR signal in 2I lines. For half-integer spin nuclei (^{7}Li, ^{23}Na, ^{39}K: I = 3/2; ^{27}Al: I = 5/2; ^{133}Cs: I = 7/2) , only the central band (m = $-1/2 \rightarrow$ m = +1/2 transition) is observed in the presence of a strong quadrupolar interaction (Smith & van Eck, 1999). When this interaction becomes significant with respect to the spin system interaction with the external magnetic field, the central line is shifted and broadened by second-order effects that are not cancelled by magic angle spinning. To obtain high-resolution solid-state NMR spectra, appropriate mechanical devices (DOR, DAS) or pulse sequences are required to eliminate the second-order perturbations (Smith & van Eck, 1999). The most recent ones, proposed initially by Frydman's group (Medek *et al.*, 1995), are based on a pulse sequence that correlates a symmetric multiple quantum coherence (m = $-3/2 \rightarrow$ m = +3/2) with the single quantum transition (m = $-1/2 \rightarrow$ m = +1/2) of the quadrupolar nucleus. To improve this basic 2D MQMAS (multiple quantum magic angle spinning) experiment, several pulse sequences have been published since, and they were summarized in a recent paper (Pruski *et al.*, 2000).

MATERIALS AND METHODS

Synthetic saponites with 0.30, 0.35, 0.40, 0.5, 0.6 and 0.75 charge per half unit cell were prepared as described previously. Full details of hydrothermal synthesis and characterization of saponites are reported in the literature (Bergaoui *et al.*, 1995). To remove most of the water, the clays were dried at ~90ºC for one day, and then equilibrated at room temperature. The chemical formula of these saponites is $Na_{1-x}Mg_3(Si_{3+x}Al_{1-x})O_{10}(OH)_2.nH_2O$ per half unit cell. Laponite RD (Laporte organics, UK) a synthetic hectorite with a layer charge of 0.28 per half unit cell (Grandjean & Robert, 1999) was used as received. The negative charge of the investigated minerals is compensated with Na^+ counterions. ^{1}H, ^{29}Si, ^{27}Al MAS NMR spectra (4 mm zirconia rotors) and ^{23}Na 2D MQMAS spectra (2.5 mm zirconia rotors) were recorded on a Bruker Avance DSX 400WB spectrometer (B_0 = 9.04 T) working at the Larmor frequencies of 400.00, 79.50, 104.27, and 105.95 MHz, respectively. Quantitative ^{29}Si and ^{27}Al NMR MAS spectra (spinning rate of 5 and 14 kHz, respectively) were measured with single-pulse (4.25 and 2.8 µs, respectively) experiments and appropriate interpulse delays (145 s and 0.3 s, respectively). Deconvolution of the ^{29}Si NMR spectra of saponites was performed by assuming Gaussian lineshape. Similar results were also obtained from ^{29}Si NMR cross polarization (CPMAS) experiments with a delay time of 5 s. ^{1}H MAS NMR spectra were obtained by single-pulse (3.0 µs) experiments separated by an interpulse delay of 5.0 s. The rotor was spun at a rate of 13 kHz. Lorentzian lineshape was used for deconvolution except for the clay hydroxyl group peak (30% Lorentzian, 70% Gaussian). ^{23}Na 2D MQMAS spectra were recorded with a three-pulse sequence (2.20, 0.9 and 12 µs), a Z-filter (Amoureux *et al.*, 1996), and a rotation-synchronized acquisition at the sample spinning rate of 25 kHz.

RESULTS AND DISCUSSION

Structural nuclei

We first compared the NMR data with the expected clay characteristics. With the synthetic

saponites, the ^{27}Al NMR spectra (Table 1) show one Al^{IV} signal. A progressive increase of the line width is observed with the clay charge, as would be expected from a wider distribution of Al sites. A 2D 3QMAS NMR experiment did not resolve different Al environments, however. On the other hand, the duration (8 days or 4 weeks) of the hydrothermal treatment used to prepare saponites (Bergaoui *et al.*, 1995) does not change the ^{27}Al NMR spectrum significantly.

The ^{29}Si NMR spectrum of Laponite RD exhibits two signals at −94.1 and −84.5 ppm, in agreement with data from the literature (Mandair *et al.*, 1990). The main signal accounts for Si nuclei at the centre of a SiO_4 tetrahedron bound to three SiO_4 tetrahedra via bridging oxygen atoms. Silicon nuclei are deshielded by next neighbour nuclei in the octahedral sheet in which Li(I) nuclei substitute for Mg(II), accounting for the weak signal.

For the saponites studied, three ^{29}Si chemical shift ranges were detected, depending on the next nearest neighbour nuclei. Decreasing the electron density on the oxygen atoms of the silicon tetrahedron results in a more positive chemical shift, as induced by a bound Al ion. The ^{29}Si NMR spectra were decomposed into their individual components. The calculated chemical shifts are reported in Table 2, together with the Si/Al ratios deduced from the expected chemical formulae and from equation:

$$\mathrm{Si/Al} = \sum_{0}^{n} I(\mathrm{Si} - n\mathrm{Al}) / \sum_{0}^{n} I(\mathrm{Si} - n\mathrm{Al}) n/3 \qquad (1)$$

with n = 0, 1, 2, 3 ($Q_3 \rightarrow Q_0$) and I the NMR signal areas.

The chemical shift data are in the usual range for trioctahedral phyllosilicates (Kinsey *et al.*, 1984; Sanz & Robert, 1992). The lowest-charge saponite (0.30) exhibits two signals at high field and the experimental Si/Al ratio is too high for the expected charge (Table 2). This clay will not be considered further. The small residual peak at −96.7 ppm of saponite (0.35) does not affect the Si/Al ratio significantly. The good agreement with the expected Si/Al values substantiates the spectral conditions used (Table 2). These saponites were prepared by hydrothermal treatment for four weeks (Bergaoui *et al.*, 1995). After a shorter period of 8 days, the ^{29}Si chemical shifts and Si/Al ratios were found to be similar to those of the final products (Table 2).

Counterion nuclei

The main purpose of this work was to characterize Na^+ counterions. The high quadrupolar moment of ^{23}Na nucleus results in a large quadrupolar splitting, and only the central transition (m = 1/2, m = −1/2) is observed (Smith & van Eck, 1999). Second-order perturbations that are not suppressed by magic angle spinning, shift and broaden the signal, and 2D 3QMAS experiments are used to cancel such effects. For a 3/2 spin nucleus such as ^{23}Na, this experiment correlates the triple quantum coherence (symmetric) (m = −3/2 → m = +3/2) to the (m = −1/2 → m = +1/2) single quantum transition. At specific times, the anisotropic parts of the quadrupolar interaction on these transitions are refocused and an echo forms (Smith & van Eck, 1999).

TABLE 1. Chemical shift and half bandwidth of ^{27}Al MAS NMR spectra of saponites.

Clay (charge)	δ (ppm)*	Half bandwidth (Hz)
Saponite (0.35)	63.0	500
Saponite (0.40)	61.9	560
8 days	62.1	530
Saponite (0.50)	64.5	690
8 days	64.6	630
Saponite (0.60)	64.2	810
Saponite (0.75)	64.2	1160

* relative to Al^{3+}_{aq} 1 M

TABLE 2. Chemical shifts δ and Si/Al ratios deduced from the chemical formulae (calc) and the ^{29}Si MAS NMR spectra (expt) of saponites.

Clay (charge)	δ (ppm)* (0Al)	(1Al)	(2Al)	Si/Al ratio calc	expt
Saponite (0.30)	−96.9 −94.2	−89.1	——	12.3	16.0
Saponite (0.35)	−96.7 −94.2	−89.1	——	10.4	10.8
Saponite (0.40)	−94.3	−89.4	——	9.00	9.51
8 days	−94.6	−89.7	——	9.00	9.87
Saponite (0.50)	−93.5	−89.9	−84.3	7.00	6.60
8 days	−94.1	−89.1	−84.7	7.00	6.85
Saponite (0.60)	−93.1	−88.2	−84.0	5.67	5.53
Saponite (0.75)	−92.3	−87.6	−83.3	4.33	4.38

* relative to TMS

For ^{23}Na nuclei, the quadrupolar-induced shift δ_{qis} from second-order perturbations is related to the quadrupolar product P_Q as (Fernandez *et al.*, 1997):

$$\delta_{qis}\ (\text{ppm}) = -0.025 \times 10^6\ P_Q^2/\nu_0^2 \qquad (2)$$

with ν_0 the Larmor frequency. The quadrupolar product P_Q is:

$$P_Q = (e^2qQ/h)(1 + \eta^2/3)^{1/2} \qquad (3)$$

with eq the electric field gradient at the nucleus site, eQ the electric quadrupolar moment of the nucleus, and η the asymmetry parameter. A typical 2D 3QMAS NMR spectrum is shown for a saponite with 0.5 charge per half unit cell (Fig. 1).

The investigated clays exhibit only one main contour signal, except for the highest-charged saponite (Fig. 2). In this latter case, the contour plot is much more widely distributed in both dimensions, indicating a more complex situation. Such an observation has been observed for samples from two different syntheses, and this precludes any artefact during their preparation. Conversely, one mean Na^+ counterion environment is observed with the other clays.

Is the water content responsible for the unexpected behaviour obtained with saponite with 0.75 charge per half unit cell? Indeed, re-hydration of a dried kanemite sample leads to a broadening of the ^{23}Na 2D 3QMAS NMR spectrum in both dimensions (Hanaya & Harris, 1998). The relative water content of our samples has been determined by ^{1}H MAS NMR. The broad water signal intensity near 4 ppm is referenced to that of the clay hydroxyl at ~0.5 ppm (Alba *et al.*, 2000). The lack of variation (76%, 73% and 74% with saponite of 0.75, 0.50 and 0.35 interlayer charge, respectively) rules out such an explanation. More recently, the surface energetic heterogeneity of similar synthetic Na-saponites has been reported. A break of different properties (mean size, for instance) occurs for saponites with an interlayer charge in the 0.65–0.75 range per half unit cell (Michot & Villérias, 2002). In such saponites, all the ditrigonal cavities contain at least one Al atom substituting for Si, and the mean arrangement could be perturbed as an effect of counterion repulsion, for instance. Contrasting results were also observed with suspensions of lithiated saponites of 0.35 and 0.75 charge per half unit cell. With the lowest-charged clay, the ^{7}Li quadrupolar splitting increases with the clay content, as expected with ordering of clay platelets. The opposite behaviour is observed with the other Li-exchanged clay. Fast exchange between two mean interfacial sites may explain such behaviour with the highest-charged clay (Grandjean & Robert, 1999).

Under the conditions used, the projections of the gravity centre on the F_1 (vertical) and F_2 (horizontal) axes are correlated with the isotropic chemical shift δ_{iso} and the quadrupolar-induced shift δ_{qis} as:

$$\delta_{F1}\ (\text{ppm}) = \delta_{iso} - (10/17)\delta_{qis} \qquad (4)$$
$$\delta_{F2}\ (\text{ppm}) = \delta_{iso} + \delta_{qis} \qquad (5)$$

and $P_Q = 0.282\ (\delta_{F1} - \delta_{F2})$ at an external magnetic field of 9.4 T.

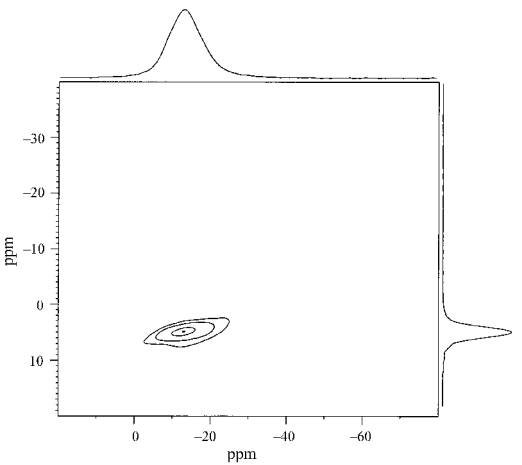

FIG. 1. ^{23}Na 2D 3QMAS spectrum of the saponite with 0.5 charge per half unit cell.

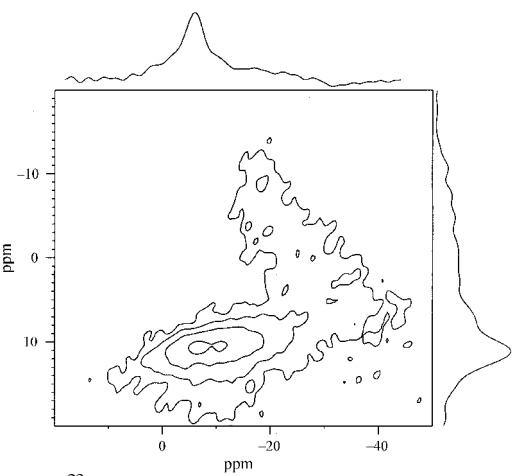

FIG. 2. ^{23}Na 2D 3QMAS spectrum of the saponite with 0.75 charge per half unit cell.

The isotropic chemical shift is a useful probe to define the nature and number of next nearest neighbour nuclei. Its value also depends on the structure of the surroundings, e.g. the O–T–O angle. The second-order quadrupolar effect that is common with nuclei such as ^{23}Na or ^{27}Al shifts the position of the broadened signal(s) in the 1D MAS NMR spectrum. Thus, this precludes any precise empirical relationship between the peak position and any structural parameter. On the other hand, the quadrupolar product P_Q is related to the electric field gradient generated at the nucleus site by its surroundings: an environment which is less symmetrical enhances this parameter, and the quadrupolar interaction.

The calculated values of the quadrupolar products and the isotropic chemical shifts are reported for saponites (Table 3). Under similar conditions, a value of 1.6 MHz was also determined for the quadrupolar product of Laponite RD. A negative charge associated with cation replacement in the tetrahedral layer can be distributed over just the three surface oxygens of one tetrahedron. Such a localized charge found in saponites induces a strong interaction of the clay with water molecules and counterions, compared to the diffuse charge brought by cation substitution in the octahedral layer (Laponite RD). Accordingly, near tetrahedral substitution sites, Na^+ cations form strong inner-sphere surface complexes. More loose outer-sphere complexes are associated with substitution in the octahedral layer (Sposito & Prost, 1982; Boek *et al.*, 1995; Greathouse & Sposito, 1998). The higher symmetry of the counterion environment reduces the electric field gradient and the quadrupolar product (the effect of the asymmetry parameter η is small, 15% at most). Thus, this can explain the significantly lower value found with Laponite. Conversely, the quadrupolar product does not change significantly with the saponite charge (Table 3).

However, a striking difference is observed with the 0.75 charge mineral (Fig. 2). The main contour signal of the highest-charged saponite provides a quadrupolar product similar to that of the other saponites (Table 3).

The 1D spectrum of the isotropic F1 dimension (vertical scale) exhibits a broad unresolved shoulder centred at ~0 ppm. Similarly, the centre of the shoulder on the right side of the main signal in the F2 dimension occurs at ~–16 ppm. Thus, an absolute value of 2.2 MHz is calculated for the quadrupolar product from the above equations.

The increase of the clay charge shifts downfield the isotropic ^{23}Na NMR signal. The variation of the ^{23}Na chemical shift δ_{iso} with the clay charge per half unit cell (q) can be approximated as (correlation coefficient = 0.92; 4 points):

$$\delta = -10.7 + 18.12q$$

With a chemical shift value of ~-6 ppm, the effective charge acting on the secondary counterion site of the highest-charge saponite is estimated as ~0.26. That means this site is more distant from the clay surface.

CONCLUSION

The interlayer charge of the saponites estimated from ^{29}Si NMR spectroscopy is in agreement with the values calculated from chemical analysis. The ^{29}Si and ^{27}Al NMR spectra of saponites prepared after 8 days and 4 weeks of the hydrothermal treatment are not significantly different. The ^{23}Na 2D 3QMAS spectra show one mean interfacial Na^+ ion site for all the investigated clays; however, for

TABLE 3. ^{23}Na quadrupolar product P_Q and isotropic chemical shift δ calculated for saponites.

Clay (charge)	δ_{F1} (ppm)	δ_{F2} (ppm)	$\lvert P_Q \rvert$ (MHz)	δ_{iso} (ppm)*
Saponite (0.35)	3.0	–15.0	2.3	–3.7
Saponite (0.50)	3.5	–12.7	2.2	–1.6
Saponite (0.60)	4.2	–11.5	2.1	–1.6
Saponite (0.75)	10.5	–7.0	2.2	+4.0
	~0	~–16	~2.2	~–6

* relative to Na^+_{aq} (1 M)

the highest-charged saponite a secondary site is detected. Such behaviour could be related to the particular properties of this latter clay as recently reported.

ACKNOWLEDGMENTS

J.G. thanks the Belgian "Fonds National de la Recherche Scientifique" for a grant to purchase the solid-state NMR spectrometer.

REFERENCES

Alba M.D., Becerro A.I., Castro M.A. & Perdigón A.C. (2000) High-resolution ^{1}H MAS NMR spectra of 2:1 phyllosilicates. *Chemical Communications*, 37–38.

Alma N.C.M., Hays G.R., Samoson A.V. & Lippmaa E.T. (1984) Characterization of synthetic dioctahedral clays by solid-state silicon-29 and aluminium-27 nuclear magnetic resonance. *Analytical Chemistry*, **56**, 729–733.

Amoureux J.-P., Fernandez C. & Steuernagel S. (1996) Z-filtering in MQMAS NMR. *Journal of Magnetic Resonance A*, **123**, 116–118.

Bergaoui L., Lambert J.F., Frank R., Suquet H. & Robert J.-L. (1995) Al-pillared saponites part 3: Effect of parent clay layer charge on the intercalation-pillaring mechanism and structural properties. *Journal of the Chemical Society Faraday Transactions*, **91**, 2229–2239.

Boek E.S., Coveney P.V. & Skipper N.T. (1995) Monte Carlo molecular modelling studies of Li-, Na- and K-smectites: Understanding the role of potassium as a clay swelling inhibitor. *Journal of the American Chemical Society*, **117**, 12608–12617.

Fernandez C., Delevoye L., Amoureux J.-P., Lang D.P. & Pruski M. (1997) ^{27}Al{^{1}H} cross polarization triple-quantum magic angle spinning NMR. *Journal of the American Chemical Society*, **119**, 6858–6862.

Gevers C. & Grandjean J. (2001) A multinuclear magnetic resonance study of synthetic clays suspended in water and in dodecyldimethylamine oxide solutions. *Journal of Colloids and Interface Science*, **236**, 290–294.

Grandjean J. (2001) Interaction of a zwitterionic surfactant with synthetic clays in aqueous suspensions: A multinuclear magnetic resonance study. *Journal of Colloids and Interface Science*, **239**, 27–32.

Grandjean J. & Robert J.-L. (1999) ^{7}Li double quantum filtered NMR and multinuclear relaxation rates of clay suspensions: The effect of clay concentration and nonionic surfactants. *Journal of Magnetic Resonance*, **138**, 43–47.

Greathouse J. & Sposito G. (1998) Monte Carlo and molecular dynamics studies of interlayer structure in Li(H_2O)$_3$-smectites. *Journal of Physical Chemistry B*, **102**, 2406–2414.

Hanaya M. & Harris R.K. (1998) Two-dimensional ^{23}Na MQ MAS NMR study of layered silicates. *Journal of Material Chemistry*, **8**, 1073–1079.

Herrero C.P., Sanz J. & Serratosa J.M. (1989) Dispersion of charge deficits in the tetrahedral sheet of phyllosilicates. Analysis from ^{29}Si NMR spectra. *Journal of Physical Chemistry*, **93**, 4311–4315.

Kim Y. & Kirkpatrick R.J. (1997) ^{23}Na and ^{133}Cs NMR study of cation adsorption on mineral surfaces: Local environments, dynamics, and effects of mixed cations. *Geochimica et Cosmochimica Acta*, **61**, 5199–5208.

Kim Y., Cygan R.T. & Kirkpatrick R.J. (1996) ^{133}Cs NMR and XPS investigation of cesium adsorbed on clay minerals and related phases. *Geochimica et Cosmochimica Acta*, **60**, 1041–1052.

Kinsey R.E., Kirkpatrick R.J., Hower J., Smith K.A. & Oldfield E. (1985) High-resolution aluminium-27 and silicon-29 nuclear magnetic resonance study of layer silicates, including clay minerals. *American Mineralogist*, **70**, 537–548.

Komadel P., Madejová J., Janek M., Gates W.P., Kirkpatrick R.J. & Stucki J.W. (1996) Dissolution of hectorite in inorganic acids. *Clays and Clay Minerals*, **44**, 228–236.

Lambert J.F., Prost R. & Smith M.E. (1992) ^{39}K solid-state NMR studies of potassium tecto- and phyllosilicates: The in situ detection of hydratable K^{+} in smectites. *Clays and Clay Minerals*, **40**, 253–261.

Laperche V., Lambert J.F., Prost R. & Fripiat J.J. (1990) High-resolution solid-state NMR of exchangeable cations in the interlayer surface of a swelling mica: ^{23}Na, ^{111}Cd, and ^{133}Cs vermiculites. *Journal of Physical Chemistry*, **94**, 8821–8831.

Luca V., Cardile C.M. & Meinhold R.H. (1989) High-resolution multinuclear NMR study of cation migration in montmorillonite. *Clay Minerals*, **24**, 115–119.

Mandair J.-P.S., Michael P.J. & McWhinnie W.R. (1990) ^{29}Si MAS NMR investigations of the thermochemistry of laponite and hectorite. *Polyhedron*, **9**, 517–525.

McKenzie K.J.D. & Meinhold R.H. (1994) The thermal reactions of synthetic hectorite studied by ^{29}Si, ^{25}Mg and ^{7}Li magic angle spinning nuclear magnetic resonance. *Thermochimica Acta*, **232**, 85–94.

Medek A., Harwood J.S. & Frydman L. (1995) Multiple-quantum magic-angle spinning NMR: A new method for the study of quadrupolar nuclei in solids. *Journal of the American Chemical Society*, **117**, 12779–12787.

Michot L.J. & Villiéras F. (2002) Assessment of surface energetic heterogeneity of synthetic Na-saponites. The role of layer charge. *Clay Minerals*, **37** 39–57.

Pruski M., Wiench J.W. & Amoureux J.P. (2000) On the conversion of triple- to single-quantum coherences in MQMAS NMR. *Journal of Magnetic Resonance*, **147**, 286–295.

Sanz J. & Serratosa J.M. (1984) ^{29}Si and ^{27}Al high-resolution NMR spectra of phyllosilicates. *Journal of the American Chemical Society*, **106**, 4790–4793.

Sanz J. & Robert J.-L. (1992) Influence of structural factors on ^{29}Si and ^{27}Al NMR chemical shifts of phyllosilicate s 2:1. *Physics and Chemistry of Minerals*, **19**, 39–45.

Schroeder P.A. & Pruett R.J. (1996) Fe ordering in kaolinite: Insights from ^{29}Si and ^{27}Al MAS NMR spectroscopy. *American Mineralogist*, **81**, 26–38.

Smith M.E. & van Eck E.R.H. (1999) Recent advances in experimental solid state NMR methodology for half-integer spin quadrupolar nuclei. *Progress in Nuclear Magnetic Resonance Spectroscopy*, **34**, 159–201.

Sposito G. & Prost R. (1982) Structure of water adsorbed on smectites. *Chemical Reviews*, **82**, 553–572.

Tkáč I., Komadel P. & Müller D. (1994) Acid-treated montmorillonites – A study by ^{27}Si and ^{29}Al MAS NMR. *Clay Minerals*, **29**, 11–19.